

Supporting Information

Facile Yolk-shell mesoporous silica nanoparticles for targeting tumor therapy

Liangliang Dai, Qingfeng Zhang, Hao Gu, Kaiyong Cai*

Key Laboratory of Biorheological Science and Technology, Ministry of Education,
College of Bioengineering, Chongqing University, Chongqing 400044, P. R. China

*Corresponding author: Prof. Kaiyong Cai

College of Bioengineering

Chongqing University

Chongqing 400044

P. R. China

Tel: +86-23-65102507

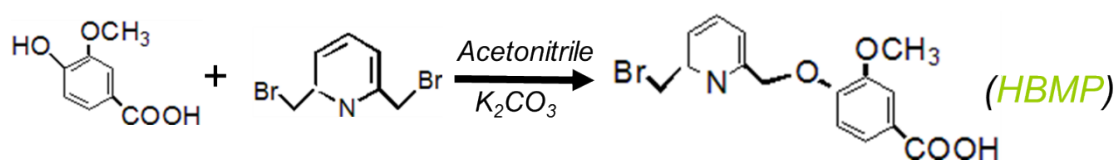
Fax: +86-23-65102877

E-mail: kaiyong_cai@cqu.edu.cn

List of Contents

Figure S1. Synthesis process and chemical structure of HBMP and PDR -----	S3
Figure S2. Size distributions -----	S4
Figure S3. Physical property characterizations -----	S5
Figure S4. FTIR spectra of different YMSN -----	S6
Figure S5. NMR spectra of different YMSN -----	S9
Figure S6. Quantification analysis of endocytosis -----	S12
Figure S7. Flow cytometry analysis -----	S13
Figure S8. Energy dispersive spectrometer analysis -----	S14
Figure S9. XPS analysis -----	S15
Figure S10. The hemolysis assays -----	S16
Table S1. BET and BJH parameters of different YMSN -----	S17
Table S2. Zeta-potential measurements -----	S18
References -----	S19

A



B

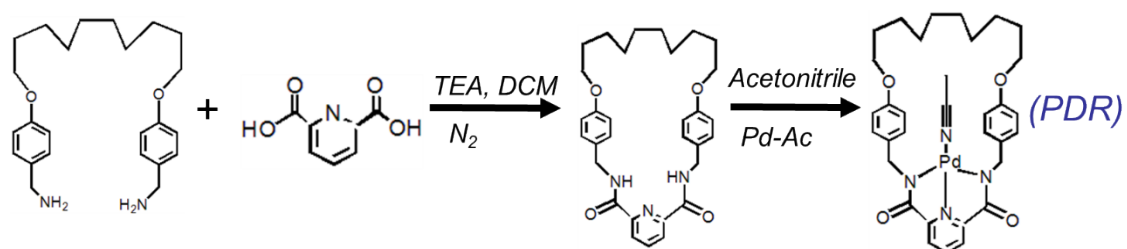
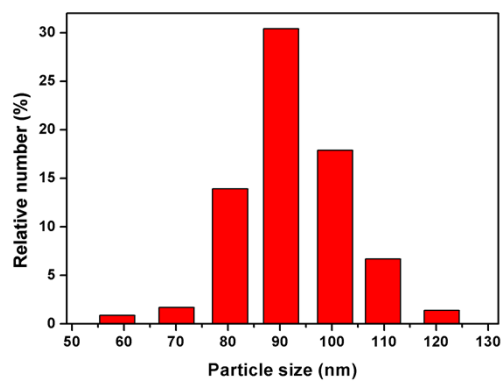


Figure S1. The synthesis process and chemical structure of (A) HBMP and (B) PDR.

A



B

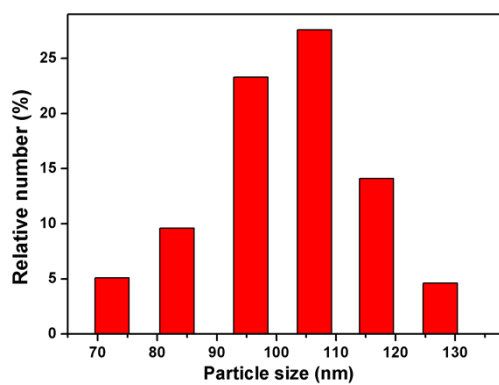


Figure S2. Particles size distributions of YMSN (A) and YMSN-HBMP-PDR-FA (B) nanoparticles via dynamic light scattering (DLS) analysis.

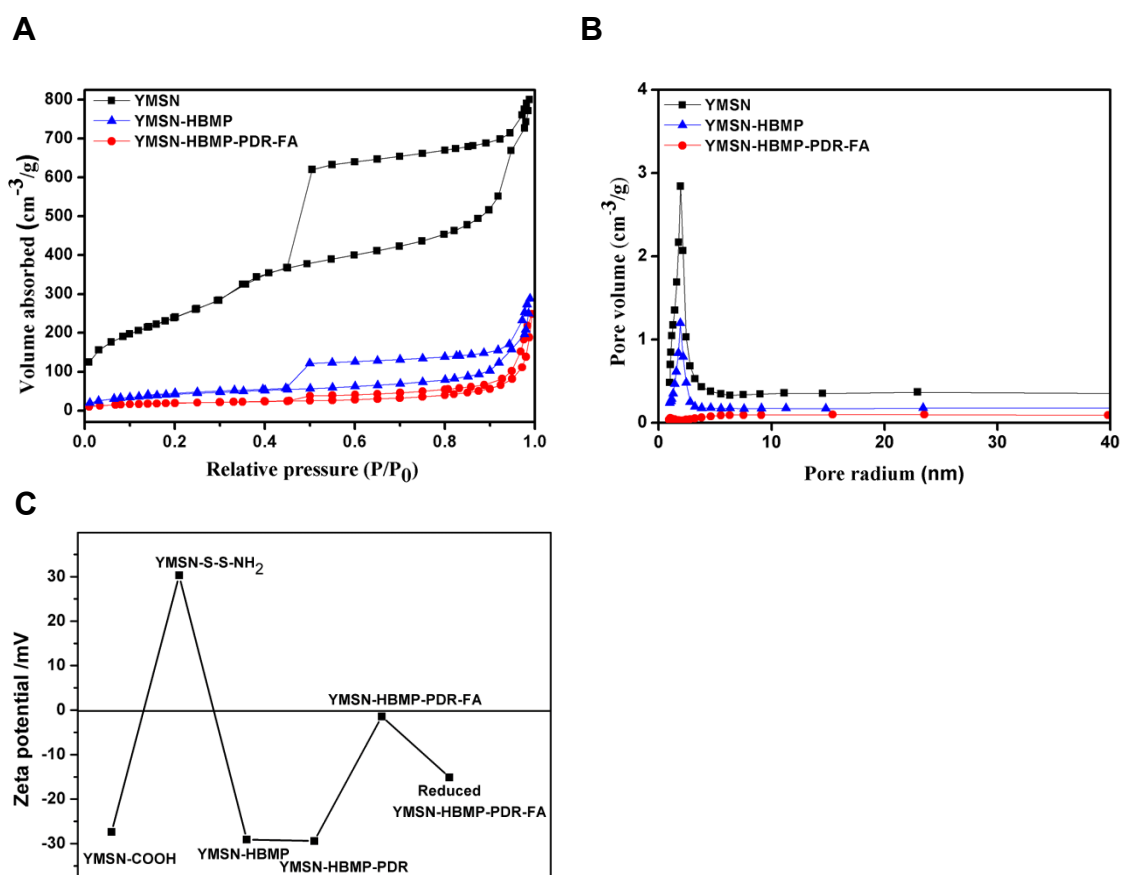


Figure S3. Physical property characterizations: (A) pore size (B) and volume distribution and (C) zeta potential values of various functionalized YMSN, respectively.

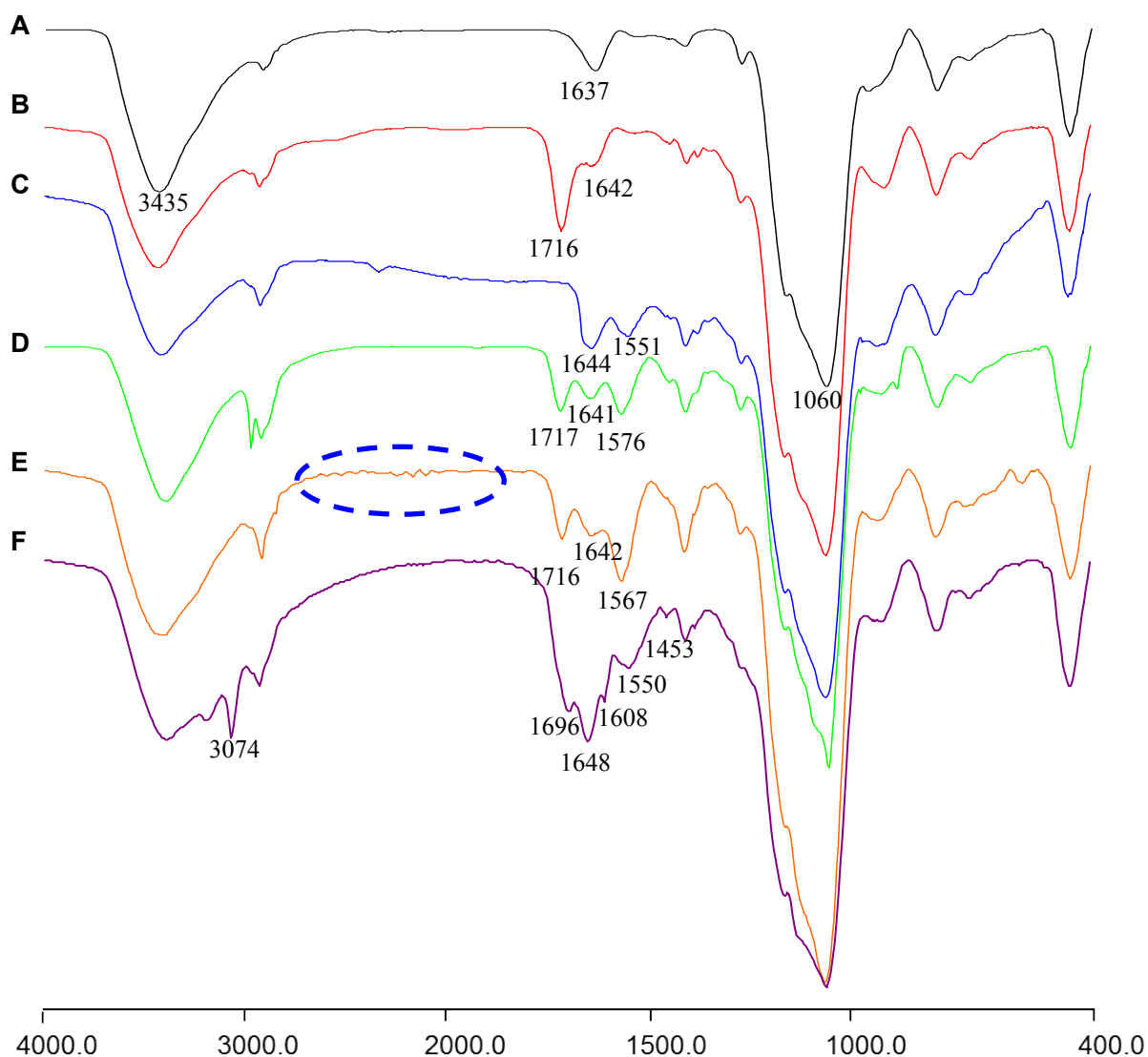


Figure S4. FTIR spectra of (A) YMSN, (B) YMSN-COOH, (C) YMSN-S-S-NH₂, (D) YMSN-HBMP, (E) YMSN-HBMP-PDR, and (F) YMSN-HBMP-PDR-FA, respectively.

Figure S4 shows the FTIR spectra of different substances. YMSN displayed a strong absorption signal at 1060 cm⁻¹, which was assigned to asymmetric stretching of Si-O-Si bridges. Peaks at 3431 cm⁻¹ and 1636 cm⁻¹ were attributed to physically adsorbed water molecules in YMSN (Figure S4 a). After conjugation with 3-

(triethoxysilyl) propylsuccinic anhydride (TSPSA), distinctive absorption peak at 1716 cm^{-1} (C=O) was observed (Figure S4 b), when comparing with that of YMSN. The results indicate that YMSN-COOH was successfully synthesized. After modification with cystamine dihydrochloride, the carboxyl groups signals (around 1716 cm^{-1}) were disappeared in the spectrum of disulfide bond-linked YMSN-COOH (YMSN-S-S-NH₂) (Figure S4 c). The intensities of peaks at 1644 cm^{-1} and 1551 cm^{-1} were enhanced, which was attributed to the further introduction of amide I and amide II groups after reacting with cystamine molecules. The results indicate that disulfide bonds were covalently conjugated to YMSN.

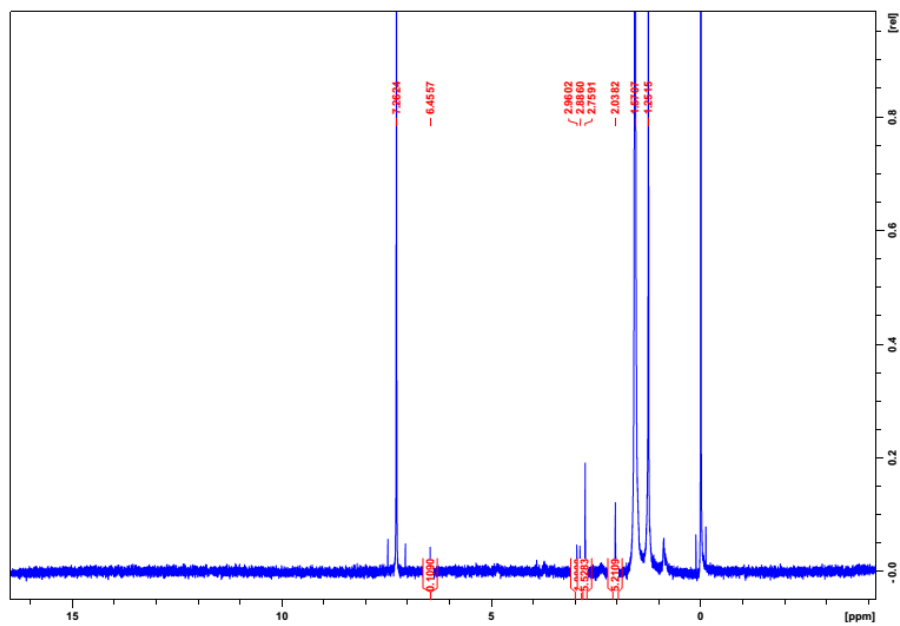
For YMSN-HBMP (Figure S4 d), a discernable peak at 1697 cm^{-1} (C=O) was observed when comparing to YMSN-S-S-NH₂. Moreover, the amide I and amide II peaks of YMSN-HBMP slightly shifted from 1644 cm^{-1} and 1551 cm^{-1} to 1641 cm^{-1} and 1576 cm^{-1} , respectively. The results suggest that the YMSN-HBMP was successfully fabricated.

After modification with Pd template rotaxane ligand (PDR), the overtone bands appearing at the range of $2800\text{-}1800\text{ cm}^{-1}$ (dash circle) were observed, which was assigned to the benzene derivative molecules deriving from PDR. The result was consistent with previous studies.^{S1, S2} Furthermore, the C=O and amide peaks of YMSN-HBMP-PDR (Figure S4 e) were slightly shifted to 1716 cm^{-1} , and 1642 cm^{-1} , 1567 cm^{-1} , respectively. The results imply that the PDR molecules were covalently conjugated to YMSN-HBMP-PDR molecules.

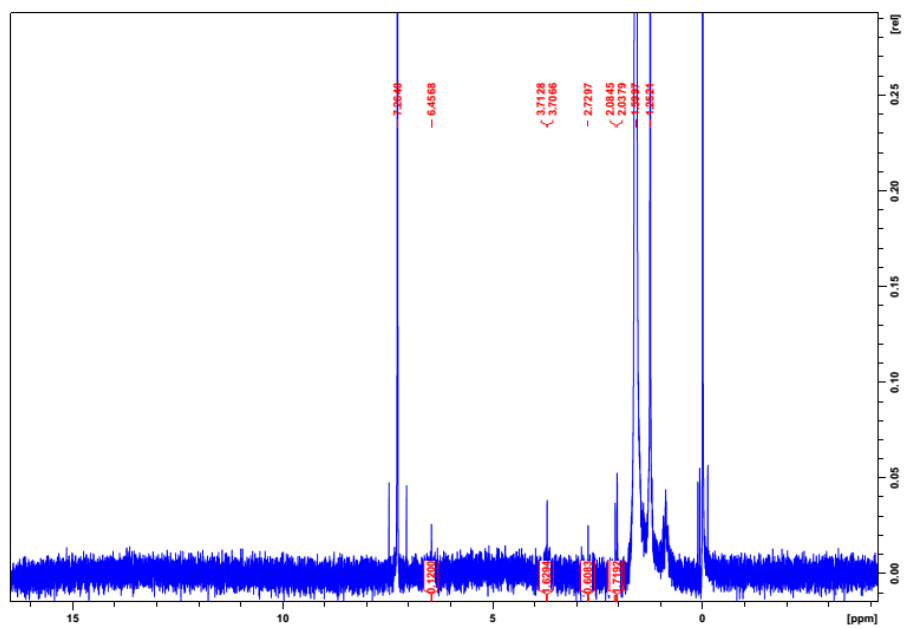
After reaction with FA, the peak at 1453 cm^{-1} was assigned to the stretching of

benzyl groups in the FA unit (Figure S4 f), which was consistent with previous studies.^{S3, S4} Meanwhile, the C=O peak of YMSN-HBMP-PDR-FA obviously shifted from 1716 cm^{-1} to 1696 cm^{-1} , owing to the introduction of C=O group derived from FA. The distinctive absorption peak at 3074 cm^{-1} was contributed to the stretching of -OH groups from FA. The distinctive absorption peak at 1608 cm^{-1} was derived from the C–N stretching of the $-\text{C}(\text{NH}_2)$ groups of FA molecules, which was consistent with a previous report.^{S5} Moreover, the amide peaks of YMSN-HBMP-PDR-FA was significantly shifted to 1648 cm^{-1} and 1550 cm^{-1} , owing to the introduction of ethylenediamine between YMSN-HBMP-PDR and FA. It demonstrates that the YMSN-HBMP-PDR-FA was successfully synthesized.

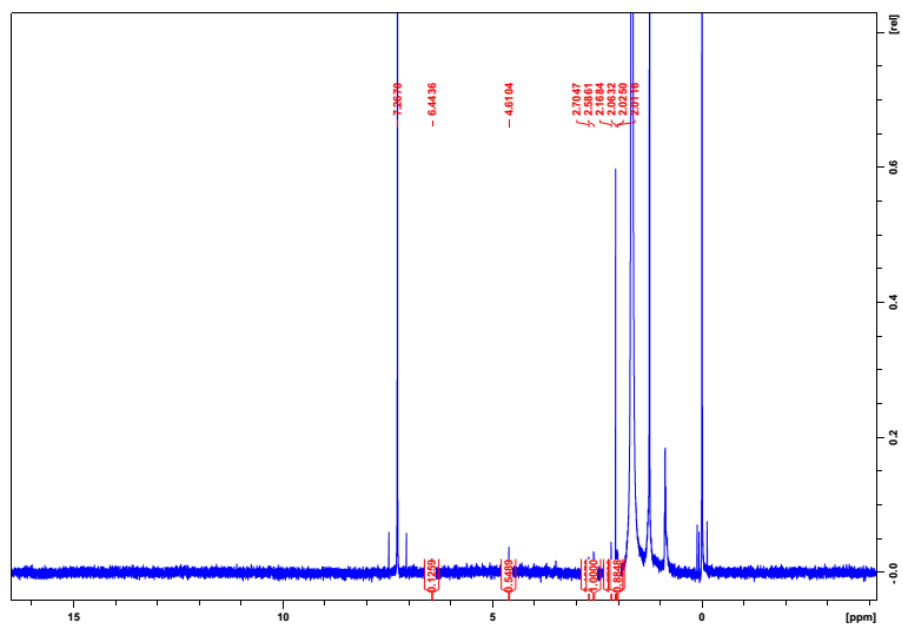
A



B



C



D

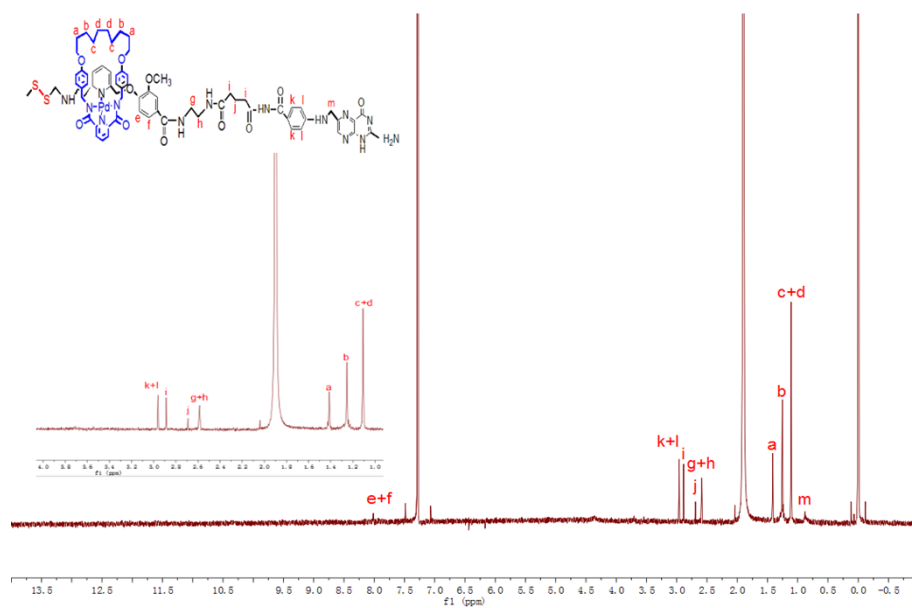


Figure S5. ^1H NMR spectra (400 MHz, CDCl_3) of (A) YMSN-S-S-NH₂, (B) YMSN-HBMP, (C) YMSN-HBMP-PDR, and (D) YMSN-HBMP-PDR-FA, respectively.

For YMSN-S-S-NH₂, distinctive peaks at 2.75-2.96 (2H), and 2.03 (2H) ppm were observed (Figure S5 a). Those peaks were attributed to the introduction of cystamine dihydrochloride molecules, which was consistent with a previous report.⁵⁶ After further coupling with HBMP, significant absorption peaks at 3.7-3.71 were observed and assigned to the linker between YMSN-S-S-NH₂ and HBMP. Moreover, distinctive peaks of 2.72, 2.03-2.08 and 4.31 ppm were observed when comparing with YMSN-S-S-NH₂ (Figure S5 b), which was attributed to the introduction of HBMP. Furthermore, after modification with PDR, the peak at 4.61 ppm was assigned to the newly formed linkage between YMSN-HBMP and PDR. While the distinctive peaks of 2.01-2.16 and 2.68-2.7 ppm were noticed and assigned to the introduction of PDR (Figure S5 c). The result suggests that YMSN-HBMP-PDR was successfully synthesized. Finally, after reaction with FA, the peak at 2.56 was assigned to the covalent bond linker between YMSN-HBMP-PDR and folic acid molecules. Furthermore, the distinctive peaks at 0.86 (m), 2.67 (i), 2.86 (j) were attributed to the conjugated FA molecules (Figure S5 d).

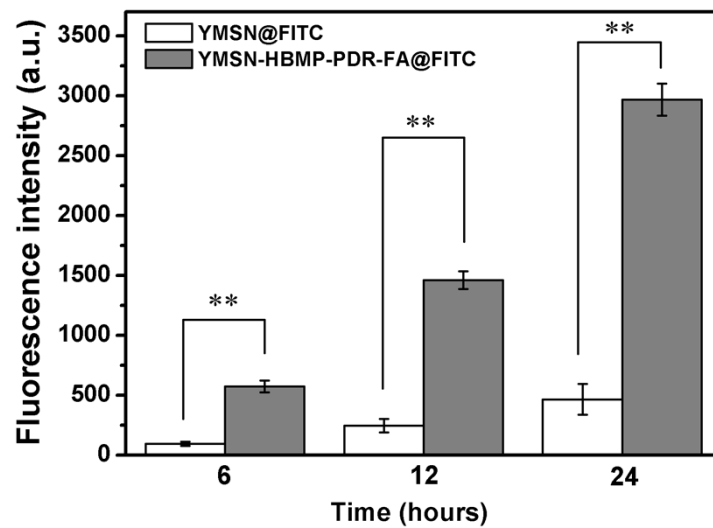
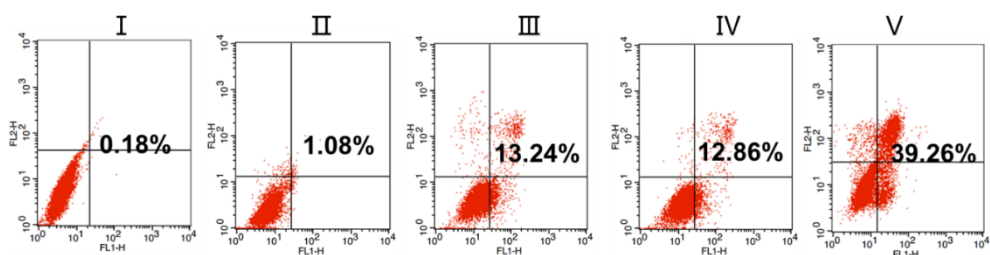


Figure S6. The quantification analysis of nanoparticles in HepG2 cells after treating with YMSN@FITC and YMSN-HBMP-PDR-FA@FITC (0.286 mg/mL) for 6, 12 and 24 h, respectively. Error bars represent means \pm SD (n=4), **p < 0.01.

A



B

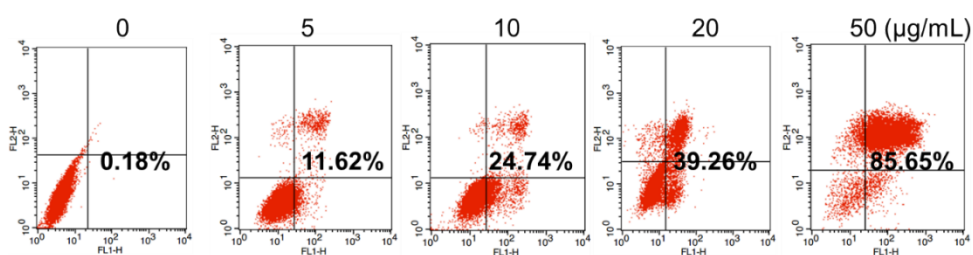


Figure S7. (A) Flow cytometry analysis of HepG2 cells after culture with PBS (control, I) and incubation with 0.286 mg/mL of YMSN (II), 20 µg/mL of DOX (III), YMSN@DOX (0.286 mg/mL,IV) and YMSN-HBMP-PDR-FA@DOX (0.286 mg/mL, V) at 37 °C for 24 h; and (B) Flow cytometry analysis of HepG2 cells apoptosis after culture with various concentrations of YMSN-HBMP-PDR-FA@DOX for 24 h.

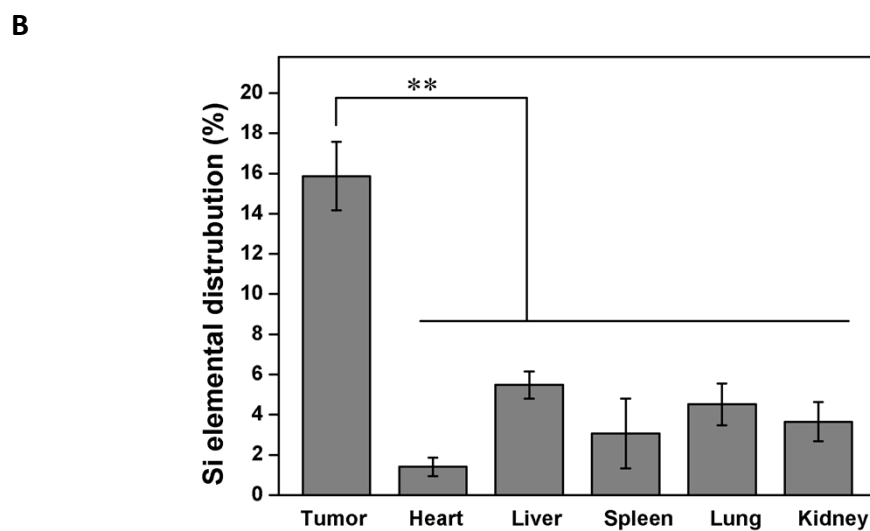
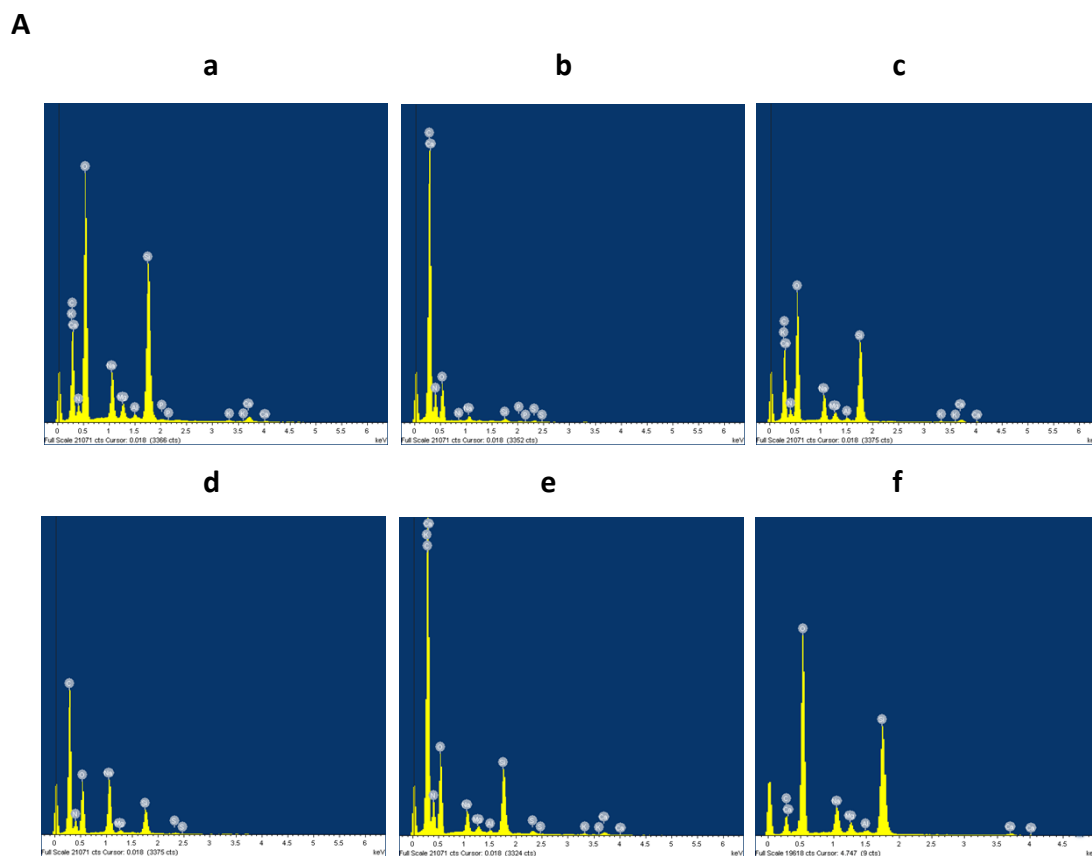


Figure S8. Energy dispersive spectrometer analysis (A and B) of Si element in major organs/tissues (a: tumor, b: heart; c: liver; d: spleen; e: lung and f: kidney) of mice after treatment with YMSN-HBMP-PDR-FA@DOX for 20 days, respectively. Error bars represent means \pm SD (n=3), **p < 0.01.

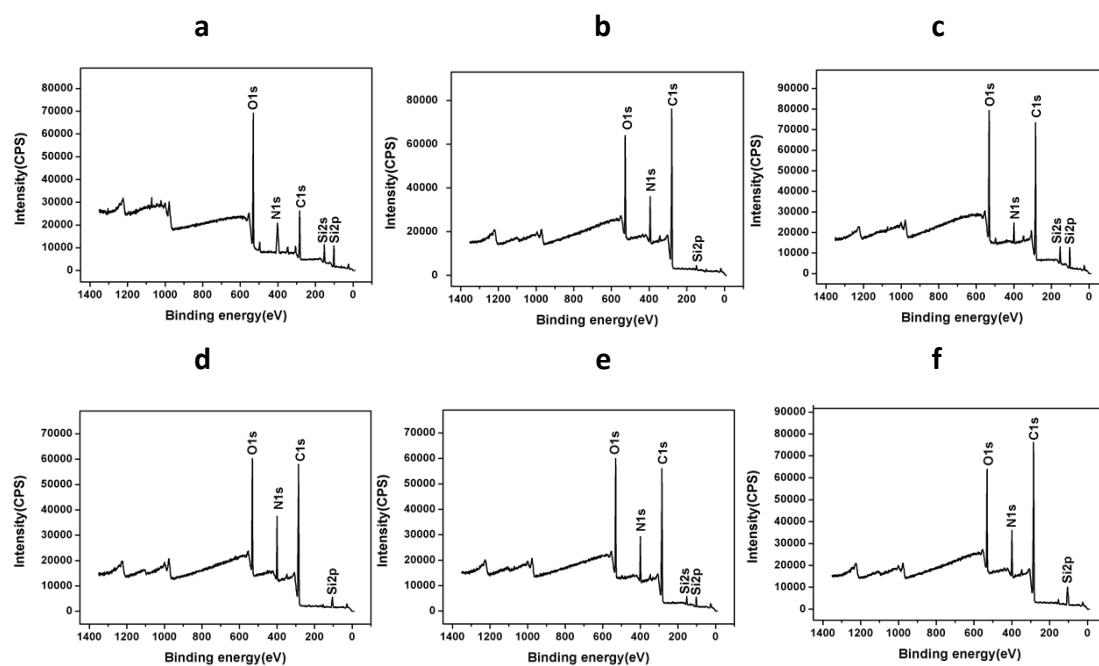
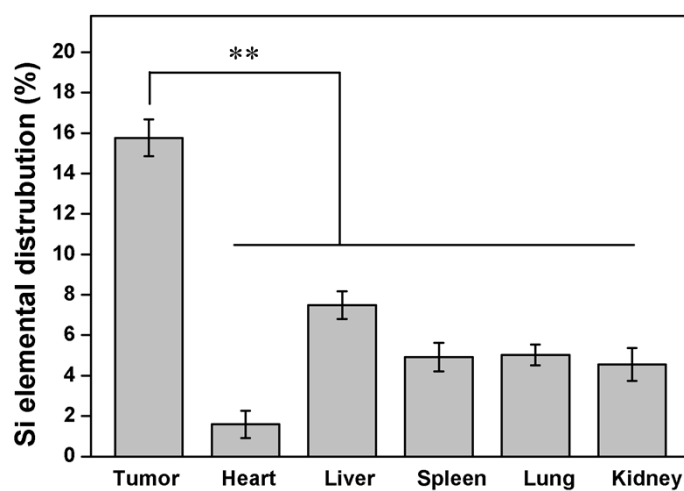
A**B**

Figure S9. The quantitative Si X-ray photoelectron spectroscopy analysis (A and B) of major tissues/organs (a: tumor, b: heart; c: liver; d: spleen; e: lung and f: kidney) of mice after treatment with YMSN-HBMP-PDR-FA@DOX for 20 days, respectively. Error bars represent means \pm SD (n=3), **p < 0.01.

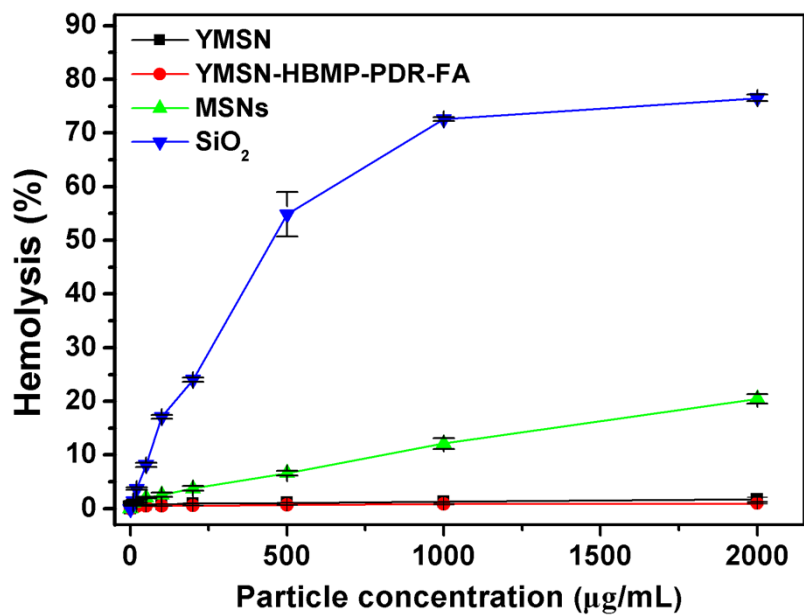


Figure S10. The hemolysis assays of RBCs treated with difference nanoparticles within various concentrations.

Table S1. BET and BJH parameters of YMSN, YMSN-HBMP and YMSN-HBMP-PDR-FA nanoparticles.

Materials	S_{BET} (m ² /g)	V_{P} (cm ³ /g)	BJH W_{BJH} (Å)
YMSN	877.2836	1.124519	51.2728
YMSN-HBMP	157.8842	0.303856	35.8643
YMSN-HBMP-PDR-FA	69.7002	0.12229	16.4662

Table S2. Zeta potentials of different nanoparticles.

Materials	Zeta potential (mV)
YMSN-COOH	-27.4±4.41
YMSN-S-S-NH ₂	30.3±4.47
YMSN-HBMP	-29.1±3.06
YMSN-HBMP-PDR	-29.4±2.28
YMSN-HBMP-PDR-FA	-1.396±0.86
Reduced YMSN-HBMP-PDR-FA	-15.1±2.24

References

- S1. J. Sienkiewicz-Gromiuka, H. Głuchowskaa, B. Tarasiukb, L. Mazura, Z. Rzączyńskaa, *J. Mol. Struct.*, 2014, **1070**, 110-116.
- S2. H. Gökce, S. Bahçeli, *Spectrochim. Acta, Part A.*, 2011, **78**, 803-808.
- S3. R. Kitaura, G. Onoyama, H. Sakamoto, R. Matsuda, S. Noro, S. Kitagawa, *Angew. Chem. Int. Ed. Engl.*, 2004, **43**, 2684-2687.
- S4. A. Mederos, S. Domínguez, S. Hernández-Molina, S. Sanchiz, F. Brito, *Coord. Chem. Rev.*, 1999, **193**, 857-911.
- S5. G. F. Li, D. Magana, R. B. Dyer, *J. Phys. Chem. B.*, 2012, **116**, 3467-3475.
- S6. F. Thielbeer, S. V. Chankeshwara, E. M. V. Johansson, N. Norouzi, M. Bradley, *Chem. Sci.*, 2013, **4**, 425-431.